Published in final edited form as:
Am J Physiol Renal Physiol. 2007 May ; 292(5): F1334–F1344. doi:10.1152/ajprenal.00308.2006.

Nephrogenic diabetes insipidus in mice caused by deleting COOH-terminal tail of aquaporin-2

Peijun P. Shi[1], **Xiao R. Cao**[1], **Jing Qu**[1], **Ken A. Volk**[2], **Patricia Kirby**[3], **Roger A. Williamson**[1], **John B. Stokes**[2,4], and **Baoli Yang**[1]

[1]Department of Obstetrics and Gynecology, Carver College of Medicine, University of Iowa

[2]Department of Internal Medicine, Carver College of Medicine, University of Iowa

[3]Department of Pathology, Carver College of Medicine, University of Iowa

[4]Veterans Affairs Medical Center, Iowa City, Iowa

Abstract

In mammals, the hormonal regulation of water homeostasis is mediated by the aquaporin-2 water channel (Aqp2) of the collecting duct (CD). Vasopressin induces redistribution of Aqp2 from intracellular vesicles to the apical membrane of CD principal cells, accompanied by increased water permeability. Mutations of *AQP2* gene in humans cause both recessive and dominant nephrogenic diabetes insipidus (NDI), a disease in which the kidney is unable to concentrate urine in response to vasopressin. In this study, we generated a line of mice with the distal COOH-terminal tail of the Aqp2 deleted (*Aqp2*$^{\Delta 230}$), including the protein kinase A phosphorylation site (S256), but still retaining the putative apical localization signal (221–229) at the COOH-terminal. Mice heterozygous for the truncation appear normal. Homozygotes are viable to adulthood, with reduced urine concentrating capacity, increased urine output, decreased urine osmolality, and increased daily water consumption. Desmopressin increased urine osmolality in wild-type mice but had no effect on *Aqp2*$^{\Delta 230/\Delta 230}$ mice. Kidneys from affected mice showed CD and pelvis dilatation and papillary atrophy. By immunohistochemical and immunoblot analyses using antibody against the NH_2-terminal region of the protein *Aqp2* $^{\Delta 230/\Delta 230}$ mice had a markedly reduced protein abundance. Expression of the truncated protein in MDCK cells was consistent with a small amount of functional expression but no stimulation. Thus we have generated a mouse model of NDI that may be useful in studying the physiology and potential therapy of this disease.

Keywords

mouse; aquaporin-2; diabetes insipidus; protein trafficking; protein phosphorylation

In mammals, the regulation of water homeostasis is mediated mainly by a family of water channels called aquaporins (AQP). AQP1, the first member to be discovered (25), localizes to the apical and basolateral (21) membranes of the proximal tubule. The majority of the filtered water (90%) is reabsorbed by constitutively expressed AQP1 channels. However, the magnitude of water excretion is largely accomplished by the hormonal regulation of AQP2, which localizes to the apical membrane of the connecting tubule (CNT) in rodents and the collecting duct (CD) cells in all mammals. Vasopressin regulates AQP2 activity by binding to its G protein-coupled V_2 receptor in the basolateral membrane of the principal cells. This

Address for reprint requests and other correspondence: B. Yang, Dept. of Obstetrics and Gynecology, 463 MRF, Univ. of Iowa, 200 Hawkins Dr., Iowa City, IA 52242 (baoli-yang@uiowa.edu).

binding triggers a cAMP signaling cascade that leads to protein kinase A activation, phosphorylation of AQP2, and, ultimately, insertion of functional water channels in apical membranes (24,31). AQP2 in the apical membrane is the rate-limiting step in the flow of water across CD cells. Water entering the cell across the apical membranes exits the cell to the interstitium via AQP3 and AQP4 in the basolateral membranes. Thus the action of vasopressin is to regulate the rate-limiting step in water flow across the CD.

Mutations of *AQP2* cause autosomal dominant and recessive nephrogenic diabetes insipidus (NDI; see Refs. 3,6, and 27), a disease in which the kidney is unable to concentrate urine in response to vasopressin (10,14,23,34). In general, AQP2 mutants causing recessive NDI are misfolded, retained in the endoplasmic reticulum (ER), and are unable to interact with wild-type (WT) AQP2 (30,33). AQP2 mutants causing dominant NDI do interact with WT AQP2 but, because of the mutation, cause missorting of the WT AQP2 mutant complex (5,10,13,16,20). In contrast to mutants in recessive NDI, AQP2 mutations found in dominant NDI are all located in the COOH-terminal tail of the protein.

The COOH-terminal tail of AQP2 is of critical importance for the insertion of AQP2 in the apical membrane. The activation of protein kinase A in response to vasopressin causes phosphorylation of the Ser residue at position 256 in the COOH terminus (7,11,12,19,22). Another region critical to insertion of AQP2 in the apical membrane is a stretch of amino acids at the COOH terminal between positions N220 and S229 (4,32). There are other regions in the COOH terminus that are critical for normal AQP2 function, since several mutations in this region produce NDI in humans (5,10,13,16,20).

The current experimental data indicate that the proximal region of the COOH-terminal tail, N220–S229, is necessary but not sufficient for localization of AQP2 in the apical membrane and that the NH2- and COOH-terminal tails of AQP2 are essential for trafficking of AQP2 to intracellular vesicles and its shuttling to and from the apical membrane (32).

To understand the pathophysiology of genetic mutations in *AQP2* that lead to NDI, several groups of investigators have created mice with mutations in *Aqp2*. Four different kinds of genetic changes have been introduced to the mouse *Aqp2* gene (26,29,35,36), and an additional two spontaneous mutations have also been identified (15,17). Our approach to assessing the in vivo role of the Aqp2 COOH-terminal tail was to generate a line of mice with deletion of the distal region of the COOH-terminal tail of the Aqp2 channel (including the S256 residue) while still retaining the putative apical localization signal. We sought to answer the question of whether such a mutation would produce viable mice and whether they would have a dominant or recessive phenotype.

MATERIALS AND METHODS

Gene targeting of mouse Aqp2 gene

A 4.5-kb fragment, amplified using Aqp2f2 (5′-GAT GAC AAA ACC CGG AGA GA-3′) and Aqp2r2 (5′-TGA GGT CAA GCC ACT GTC AC-3′) as primers and mouse R1 ES cell genomic DNA as template, was subcloned into pCR2.1 (Invitrogen, Carlsbad, CA) vector to form pBYAqp2. This 4.5-kb genomic fragment contains exons 2 to 4, the entire coding sequence. pBYAqp2 was cut at the *Sbf*I site within exon 4. Mung bean nuclease digestion was used to generate blunt ends, followed by the *Nhe*I cut. IRES-Cre-ER-Neo cassette (kindly provided by Dr. P. Chambon) was obtained from the plasmid pBY53a with *Not*I, Klenow filled in, and then cut with *Nhe*I. The two fragments were ligated to form the plasmid pBYAQP3, the targeting construct. After homologous recombination, the Aqp2 peptide would be truncated right after S229, however, during subcloning, three extra amino acids (RPL) that were not present in WT Aqp2 were introduced before the stop codon.

Therefore, the predicted protein COOH-terminus would be S(229)RPL(232)X. For simplification, this truncated allele is called *Aqp2*$^{\Delta 230}$. The linearized targeting vector was electroporated into ES cells. Transfection of ES cells and selection of drug-resistant colonies was as described previously (18). ES cell screening was performed by PCR. First screening from the short homology arm side yielded a 2.5-kb PCR product: Aqp2Kif2 (5′-TCA GCC ATG ATG GAT ACT TTC TCG-3′) located within the N*eo* cassette and Aqp2KIr1: (5′-GTC ACC GAT ACC CAC TCT TCT GG-3′), located at downstream of the 3′ -short homology region.

The positive clones were confirmed from the long homology arm side: CR5′f (5′-GAA AGA CCT TGA AGC ACC ATG C-3′) located upstream of the 5′ -long arm homology region and Aqp2seqr3 (5′-TCC CTG AAC ATG TCC ATC AG-3′) located within the *IRES-Cre* knock-in cassette, to get 3.5-kb PCR product.

Two positive ES cell clones were obtained out of nearly 2,000 colonies screened. Positive clones were injected in C57BL/6 (B6) blastocytes. Male chimeras were bred to B6 and 129/SvJ females to generate mice on two different genetic backgrounds. Tail DNA from 3-wk-old agouti pups were screened for the presence of the targeted gene. Heterozygous *Aqp2* $^{\Delta 230}$ mice were backcrossed to WT B6 mice for two generations and then intercrossed to generate mice for this study. Thus our mice have mixed genetic background of B6 and 129/SvJ with predominantly B6 (on average 87.5% from B6).

Care of the mice used in the experiments met or exceeded the standards set forth by the National Institutes of Health in their guidelines for the care and use of experimental animals. All procedures were approved by the University Animal Care and Use Committee at the University of Iowa.

Genotyping and PCR

Genomic DNA was isolated from tail clips from 3-wk-old mice and used for PCR genotyping. Primers, F1 (5′-TCA GAA CTT GCC CAC TAG CC-3′), located at the 5′-homology region, and R1 (5′-GAG GAA CTG CTT CCT TCA CG-3′), located within the *IRES-Cre* cassette, amplify a 530-bp fragment for the mutant allele. Primers F1 and R2 (5′ -AGG AGG GAA CCG ATG ACG-3′), located at the 3′ -homology region, amplify a 540-bp fragment for the WT allele (Fig. 1).

Total RNA was isolated using the Sigma TRI REAGENT kit followed by DNase I treatment to remove genomic DNA from RNA preparations. First-strand cDNA was synthesized using Invitrogen SuperScript III reverse transcript and oligo(dT)20. The cDNA template then was used with Red-Taq (Sigma Chemical, St. Louis, MO) for PCR analysis or with the SYBRGreen PCR master mix kit (Applied Biosystem, Foster City, CA) for Real-time PCR analysis. Three WT control and three *Aqp2* $^{\Delta 230/\Delta 230}$ mice were used for real time RT-PCR analyses. The ABI PRISM 7000 Sequence Detection System was used for signal detection, and the relative standard curve method (gene of interest and internal control were in separate tubes) was used for data analysis. The following primer sets were used in RT-PCR and real-time PCR for Aqp1, Aqp2, Aqp3, and Aqp4, respectively: QPCR-AQP1F (5-′CT CCC TAG TCG ACA ATT CAC-3′), QPCR-AQP1R (5′-ACA GTA CCA GCT GCA GAG TG-3′), RT-Aqp2F (5′-CTC TCT CCA TTG GTT TCT CTG TTA CC-3′), RT-Aqp2R (5′-GGA ACG GGC TGG ATT CAT G-3′), RT-AQP3F (5′-GCT GTG ACC TTC GCA ATG TG-3′), RT-AQP3R (5′-CAG TGC ATA GAT GGG CAG CTT-3′), QPCR-AQP4F (5′-GAG TCA CCA CGG TTC ATG GA-3′), and QPCR-AQP4R (5′-CGT TTG GAA TCA CAG CTG GC-3′).

Serum and urine collections, chemistry, and osmolality measurements

Age- and gender-matched mice were placed in a metabolic cage to collect urine for 12–24 h, as described previously (1). Blood was collected via the retroorbital venous plexus using a microhematocrit blood tube. The samples were incubated at room temperature for 60 min and centrifuged at 13,000 rpm for 5 min, and serum was stored at −80°C. Blood urea nitrogen (BUN) and creatinine were measured using a VT250 Chemical Analyzer (Johnson & Johnson Clinical Diagnostics, Rochester, NY) at the Animal Clinical Laboratory Core Facility at the University of North Carolina at Chapel Hill. Urine and serum osmolality was measured with Micro Osmometer 3300 (Advanced Instruments, Norwood, MA). Desmopressin (dDAVP) was injected intraperitoneally at 1 (μg/kg body wt, and urine was collected every 6 h for 12 h. For the rescue experiment, weanlings (21 days old) were injected intraperitoneally with water (10% of body wt).

Histology and immunohistochemistry

Following a lethal dose of Avertin (2,2,2-tribromoethanol) anesthesia, mice were perfused with physiological saline and 3% formalin through the heart. The kidneys were postfixed with 10% zinc formalin, and paraffin-embedded kidney tissues were sectioned at a thickness of 2–3 μm. Standard hematoxylin and eosin staining and immunostaining were performed on paraffin-embedded kidney tissues. For immunohistochemistry, primary polyclonal antibodies (rabbit) anti-Aqp2 (COOH terminal, 1:500 dilution; Chemicon, Temecula, CA), anti-Aqp2 (NH_2 terminal, 1:100 dilution; Santa Cruz Biotechnology, Santa Cruz, CA), and anti-Aqp3 (COOH terminal, 1:1,000 dilution; Chemicon) were incubated with sections separately overnight at 4°C. FITC-labeled goat anti-rabbit IgG antibody was used as the secondary antibody. Nucleus was stained with ToPro-3 (1:1,000; Molecular Probes, Eugene, OR). After being stained, the sections were mounted in Vectashield Mounting medium (Vector Laboratories, Burlingame, CA). Immunofluorescent images were obtained with a Bio-Rad MRC-1024 Confocal Microscope (Bio-Rad Laboratories, Hercules, CA) using a ×60 oil objective.

Western blot

Kidney Western blots were performed as described previously (1). The antibodies directed against the NH_2- and COOH-terminal region of Aqp2 were the same as used for immunohisto-chemistry. Images were developed with Super Signal Femto (Pierce) and quantitated using the Optichemi BioImaging System.

Construction of Aqp2 vectors for stable transfection

One common forward primer (Aqp2BglII5: 5′-AGA TCT GGG AAC TCC GGT CCA TAG CG-3′) and two different reverse primers (Aqp2BglII31: 5′-AGA TCT GGC CTT GCT GCC GCG CGG CAG G-3′ and Aqp2BglII32: 5′-AGA TCT GCT CTT GGT CGA GGG GAA CAG C-3′) were used to amplify the full-length cDNA and the Aqp2 truncation, deleting the COOH-terminal 41 amino acids, respectively. The two PCR products were inserted in pCR2.1 TA cloning vector (Invitrogen). After sequencing confirmation, the two cDNA fragments were cut with *Bgl* II and subcloned into mammalian expression vector pCMV-Tag1 (Stratagene, La Jolla, CA) to form pCMV-Aqp2-31a and pCMV-Aqp2-32a, respectively.

Expression of Aqp2 in MDCK cells

MDCK cells were cultured in DMEM (Invitrogen) supplemented with 10% FBS, 100 U/ml of penicillin, and 100 (μg/ml of streptomycin at 37°C under a humidified 5% CO_2. Four micrograms of the expression constructs of the WT Aqp2 and truncated Aqp2 were transfected into MDCK cells grown subconfluently on six-well microplates (Corning,

Cambridge, MA) using Lipofectamine 2000 (Invitrogen) according to manufacturer's instructions. After 24 h, transfected cells were trypsinized and passed at a 1:10 ratio in fresh medium. The following day, cells were fed with DMEM containing 10% FBS and 700 (μg/ml of G418 (Sigma Chemical). Fourteen days after the transfection, individual colonies were selected and expanded. Empty pCMV-Tag1 vector was also transfected in MDCK cells as controls.

To detect the localization of proteins in polarized cells, transfected MDCK cells were grown on a permeable membrane (Transwell) with pore sizes of 0.4 (μm (Cell Culture Insert; Becton Dickinson Labware, Franklin Lakes, NJ). After the 3-day culture in DMEM, confluent cells were incubated for 2 h with DMEM containing 10 μM forskolin (Sigma Chemical) to induce the translocation of Aqp2 to the plasma membrane. Control cells were not treated with forskolin for comparison. The cells were then fixed for 10 min with cold methanol at room temperature, washed with PBS, and blocked with 3% BSA in PBS at 4°C overnight. Cells transfected with the WT or the mutant Aqp2 were incubated at room temperature for 1 h with the same antibody recognizing the NH_2-terminus used for tissue immunohistochemistry in PBS containing 1% BSA. Subsequent processing was similar to tissue immunohistochemistry.

Transepithelial water flow of cultured cells

Transcellular water flow (Pf) was determined by a spectroscopic method developed by Jovov et al. (9). In brief, MDCK cells were seeded on Transwells and grown for 3 days. The apical compartment of the Transwells was filled with 400 μl of 0.5× Hanks' balanced salt solution containing 30 mg/l phenol red. The basolateral solution contained 1.5 ml Hanks' balanced salt solution. After incubation for 2 h at 37°C, three aliquots of 50 μl were taken from the apical compartment of each well and diluted with 50 μl Hanks' balanced salt solution, and the absorbency at 479 nm (the isosbestic point of phenol red) was determined. Pf (in nm/s) was calculated using equations described previously (2).

Statistics and data analysis

Data analysis between different groups of animals was performed by unpaired Student's *t*-test, except data shown in Fig. 5 where ANOVA was used. The Kaplan-Meier survival curves (see Fig. 8) were analyzed using the Log Rank Test (8). We considered *P* values <0.05 statistically significant. All values are expressed as means ± SE.

RESULTS

A schematic drawing of the mouse Aqp2 water channel is shown in Fig. 1*A* . The *Aqp2* gene has 4 exons, the last of which contains the final transmembrane domain and the COOH-terminal tail. We disrupted *exon 4* with the selectable marker, Neo, and Cre recombinase as shown in Fig. 1*B*. A representative genotyping of a litter of mice obtained from heterozygous intercross is shown in Fig. 1*C*. The number of mice homozygous for the deletion ($Aqp2^{\Delta 230/\Delta 230}$) did not deviate from the expected Mendelian ratio. However, these homozygotes tended to be smaller than either heterozygous (HET) or WT littermates (Table 1). RT-PCR analyses using total RNA isolated from kidney of $Aqp2^{\Delta 230/\Delta 230}$ mice showed the presence of the fusion mRNA between Aqp2 and Cre recombinase and the absence of transcript derived from the 3′-region of exon 4 (Fig. 1*D*).

Kidney morphology and histology were obtained from mice at 4 wk old. On gross examination, kidneys from $Aqp2^{\Delta 230/\Delta 230}$ mice were enlarged with prominent hydronephrosis (Fig. 2*A*). The kidney weight, after normalized to body weight, was not significantly different between $Aqp2^{\Delta 230/\Delta 230}$ and control mice (data not shown). Under

light microscopy, the CDs were dilated; there was atrophy of the papilla, and there was diffuse interstitial fibrosis (Fig. 2*B*). In accordance with morphological changes, serum BUN level was significantly increased for Aqp2$^{\Delta 230/\Delta 230}$ mice when compared with either WT or HET mice, indicating reduced kidney function in Aqp2$^{\Delta 230/\Delta 230}$ mice (Table 1). The serum creatinine level was not different among mice with all three genotypes (Table 1).

We further characterized the expression of Aqp2 by immunohistochemistry. Two different antibodies, against either the COOH or NH_2 termini of Aqp2, gave strong signals from WT kidney (Fig. 2, *C* and *D*). As expected, the COOH-terminal-specific antibody did not detect any Aqp2 in the kidneys from *Aqp2* $^{\Delta 230/\Delta 230}$ mice, since the epitope was deleted by the truncation. To our surprise, the NH_2-terminal-specific antibody produced a very low level of Aqp2 from *Aqp2* $^{\Delta 230/\Delta 230}$ kidney (Fig. 2, *D* and *E*). In contrast to the apical localization of Aqp2 in CDs from WT mice, Aqp2 protein staining by this antibody in CDs from *Aqp2* $^{\Delta 230/\Delta 230}$ mice appeared only faintly and diffusely throughout the cytoplasm. Western blots were also used to detect the presence of the truncated form of the Aqp2 channel in the affected kidney. We were unable to detect Aqp2-specific signals in blots probed with either NH_2-or COOH-terminal-specific antibody from *Aqp2* $^{\Delta 230/\Delta 230}$ kidney (Fig. 3), although strong signals were obtained from both WT and HET kidneys. Thus Aqp2 protein abundance was much lower in kidneys from *Aqp2* $^{\Delta 230/\Delta 230}$ mice than in kidneys from WT or HET mice.

As shown in Fig. 1, kidneys from *Aqp2* $^{\Delta 230/\Delta 230}$ mice contain a fusion transcript instead of WT *Aqp2*. To assess the relative amounts of Aqp2 mRNA and the extent to which the expression of other Aqps might be altered in *Aqp2* $^{\Delta 230/\Delta 230}$ mice, we conducted real-time quantitative RT-PCR analyses. As shown in Fig. 4, there were no significant differences in mRNA abundance in any of the four Aqp isoforms tested. At the protein level, as revealed by immunohistochemistry using antibody against Aqp3, there was no significance between WT and *Aqp2* $^{\Delta 230/\Delta 230}$ mice (Fig. 2*F*). It seems that compensatory changes of the other Aqp water channels do not occur when Aqp2 is rendered defective, at least in these mice. In addition, differences in mRNA abundance of Aqp2 do not account for the striking difference in Aqp2 protein as determined by the antibody against the NH_2 terminus (Fig. 2 and Fig. 3).

Age-matched (4-wk-old) WT, *Aqp2* $^{\Delta 230/+}$ (HET), and *Aqp2* $^{\Delta 230/\Delta 230}$ mice, were used for the initial analyses of urine output. *Aqp2* $^{\Delta 230/\Delta 230}$ mice had dramatically increased urine output in 12 h compared either WT or HET mice for the truncation of Aqp2 (Fig. 5*A*). Also, the urine osmolality was lower for *Aqp2* $^{\Delta 230/\Delta 230}$ mice (193 ± 17 for *Aqp2* $^{\Delta 230/\Delta 230}$ vs. 1,093 ± 119 mosmol/kgH_2O for WT, and 1,275 ± 233 mosmol/kgH_2O for HET mice; Fig. 5*B*). There was no difference between WT and HET mice in either the amount of urine produced or the urine osmolality. These relationships were not changed when we normalized urine output for body weight to take into consideration the smaller size of the homozygotes (Fig. 5*D*). As expected, given their increased urine output, homozygotes have more than threefold greater water consumption than WT or HET (Fig. 5*E*). Consistent with expectations, the *Aqp2* $^{\Delta 230/\Delta 230}$ mice have increased serum osmolality (Fig. 5*C*). Thus mice with the COOH-terminal tail truncation of Aqp2 have diabetes insipidus. The absence of a phenotype in HET indicates that this mutation is transmitted as an autosomal recessive disorder.

We next determined the responsiveness of control and *Aqp2* $^{\Delta 230/\Delta 230}$ mice to a single dose of dDAVP (1 μg/kg body wt ip). Urine was collected for 12 h before and 12 h after injection. As shown in Fig. 6, the control mice showed a significant reduction in urine volume and an increase in urine osmolality after dDAVP. In contrast, the *Aqp2* $^{\Delta 230/\Delta 230}$ mice were resistant to dDAVP. Thus mice with the COOH-terminal tail truncation of Aqp2 have NDI.

After the initial analyses at 4 wk old, the same mice were tested again at 8 wk. As shown in Fig. 7, the amount of urine produced by control mice at 8 wk of age was more than that at 4 wk of age, but the amount was almost identical when normalized to the body weight (Fig. 7*B*). In contrast, the *Aqp2* $^{\Delta 230/\Delta 230}$ mice showed significant increase of their urine volume as follows: at 8 wk the amount of urine produced was increased more than threefold than that at 4 wk. Normalized to body weight, urine volume at 8 wk was still almost two times that at 4 wk ($P < 0.005$; Fig. 7*B*). However, as shown in Fig. 7*C* , the urine osmolality was not changed significantly between those two time points.

Aqp2$^{\Delta 230/\Delta 230}$ mice were viable and could survive to adulthood; in addition, adult *Aqp2* $^{\Delta 230/\Delta 230}$ mice, both male and female, were fertile (data not shown). However, ~40% died around the time of weaning. One likely cause for this high mortality was dehydration, since some mice demonstrated decreased body weight, increased hematocrit (data not shown), and dry appearance of the skin and fur. We tested the idea that weanling mice might have difficulty obtaining sufficient water intake by administering a single dose of sterile water (10% body wt ip) and recorded subsequent mortality. After a single injection, the survival of the homozygotes improved dramatically. All water-injected mice were still alive at 6 mo. The Kaplan-Meier survival curves for both groups of mice are shown in Fig. 8.

The apparent diffuse distribution of Aqp2Δ230 in the CDs from *Aqp2* $^{\Delta 230/\Delta 230}$ mice suggested that the apical translocation in response to vasopressin was abolished with the deletion of the COOH-terminal tail. However, the low level of expression of the truncated protein made it difficult to conduct detailed studies. As an alternative approach to determining the subcellular localization of Aqp2, we used MDCK cells stably expressing either full-length Aqp2 or Aqp2$^{\Delta 230}$. As shown in Fig. 9, *A* and *B*) for cells transfected with full-length *Aqp2* cDNA, in the absence of stimulation, Aqp2 was seen diffusely throughout the cell. In the presence of forskolin, a direct activator of adenylate cyclase for the production of cAMP, the majority of the Aqp2 was seen at the plasma membrane. For cells transfected with Aqp2$^{\Delta 230}$, the cellular distribution of truncated Aqp2 was similar to full-length Aqp2 in the absence of stimulation (Fig. 9, *A* and *C*). However, adding forskolin to the culture medium did not seem to alter the expression pattern of Aqp2$^{\Delta 230}$, which was dramatically different from that of full length Aqp2 (cf. Fig. 9, *B* and *D*), and was in agreement with the immunostaining result using the NH_2-terminal specific antibody (Fig. 2*E*).

To test if the Aqp2 channels with the Δ230 truncation still retained some functional activity, we measured transepithelial water permeability in these cells. As shown in Fig. 10, MDCK cells transfected with only an empty vector had minimal water permeability; forskolin tended to increase permeability, but the change was not statistically significant. Cells transfected with full-length Aqp2 had significantly greater water permeability in the absence of stimulation compared with MDCK cells transfected with vector. Upon treatment with forskolin, MDCK-Aqp2 cells further increased their water permeability. Cells transfected with Δ230 truncation had similar basal water permeability as MDCK cells transfected with full-length Aqp2 and greater water permeability than MDCK cells transfected with the empty vector. Stimulation with forskolin did not produce an increase of the water permeability over basal levels.

DISCUSSION

The present results describe a line of mice with severe autosomal recessive NDI from deletion of the COOH terminus of Aqp2. In contrast to some other lines of mice with mutations in Aqp2, these mice can survive to adulthood. Also in contrast to other lines of mice, the amount of Aqp2 protein is markedly diminished in the homozygous mice. The

40% mortality of the homozygous mice during the weaning period can be markedly reduced by a single dose of water. MDCK cells stably expressing the WT and COOH-terminal truncated Aqp2 protein support the conclusion that a small amount of functional truncated protein can be inserted in the apical membrane constitutively but that vasopressin does not increase protein trafficking.

We are aware of seven other lines of mice with genetically altered *Aqp2*: *1*) a knock-in T126M mutation displayed autosomal dominant NDI and perinatal lethality (35); *2*) two lines of mice expressing a floxed third exon show different phenotypes. Such mice bred with mice universally expressing Cre recombinase had perinatal lethality (26). However, when the floxed mice were crossed with a strain that excised the exon only in the CD (and not in the CNT), mice developed severe NDI but survived to adulthood (26); *3*) mice with a floxed second exon bred with a universally expressed, tamoxifen-inducible Cre recombinase had NDI and survived to adulthood (36); *4*) mice with a F204V missense mutation had recessive NDI and survived to adulthood (15); *5*) mice with the S256L missense mutation also had recessive NDI and ~ 90% mortality around the time of weaning (17); *6*) mice with a frame-shift mutation (deleting nucleotides 763–772) and inclusion of 76 amino acids from the COOH terminus of human dominant negative mutant AQP2 showed autosomal dominant NDI (29). Thus all of the mouse models with mutations in Aqp2 have NDI, some of which produce perinatal lethality.

One of the questions we addressed in this study was whether mice with a deleted Aqp2 COOH terminus would have autosomal dominant or recessive NDI. The possibility that a COOH-terminus deletion might produce autosomal dominant NDI in mice derives from the observation that mutations in human AQP2 in the COOH terminus usually produce dominant disease. These mutations produce a dominant phenotype because they encode for a AQP2 protein that is targeted to a cell compartment other than the normal pathway leading to insertion in the apical membrane. This misdirection carries with it WT AQP2 proteins (as heterotetramers), thereby preventing normal AQP2 from reaching the apical membrane. The fact that there are now two mouse models where COOH-terminal mutations (S256L and the present truncation) do not produce dominant NDI demonstrates that not all disruptions of the AQP2 COOH terminus produce dominant disease. The cases where such mutations do produce dominant NDI must result from specific interactions between normal and abnormal COOH-termini and consequent misdirection of the resulting heterotetramer (29).

Why do some lines of mice with defective Aqp2 die in the perinatal period and others survive into adulthood? We can imagine two general possibilities. First, the genetic background of mice that survive might encode for genes that act in a permissive fashion to combat the dehydration and/or the poly-uria-induced hydronephrosis caused by these severe defects. A specific example of such a possible genetic “rescue” might be other Aqps that could partially substitute for the defective Aqp2 in some circumstances. The extent to which differences in genetic background account for the survival is difficult to assess. We note that, in one study, the excision of Aqp2 increased the expression of Aqp3 (36). In other studies, mice with the S256L and mice with T126M mutations have increased Aqp2 mRNA (35) and protein (17). However, we did not find compensation by Aqp3 or any other Aqp at the mRNA and protein level (Fig. 4 and Fig. 2), and, in our homozygous mice, the endogenous protein levels of Aqp2 were greatly reduced (Fig. 2 and Fig. 3). Given our present knowledge of Aqp biology, it seems unlikely that another Aqp could substitute for Aqp2.

A second possible explanation for a difference in perinatal mortality is that the Aqp2 mutations that permit mice to survive to adulthood might allow a small amount of functional Aqp2 protein to be expressed on the apical membrane. The present study provides evidence

to support this hypothesis. MDCK cells expressing Aqp2$^{\Delta 230}$ protein have higher basal Pf values than control cells and have similar Pf values as cells expressing WT Aqp2 without stimulation (Fig. 10). This result is consistent with the idea that a small amount of Aqp2 with a deleted COOH terminus could be constitutively expressed on the apical membrane.

Data from the published reports on mice expressing genetically altered *Aqp2* are consistent with the idea that surviving mice might express a small amount of functional Aqp2 protein. Homozygous mice expressing missense mutations [T126M (lethal; see Ref. 35) and F204V (not lethal; see Ref. 15)] have demonstrable Aqp2 protein, but some of the F204V protein appears to be fully mature (i.e., processed through the Golgi), as evidenced by the presence of an endo H resistant band. In contrast, the T126M protein does not appear to have a fully mature band. These results are consistent with the idea that mice expressing the F204V mutation live into adulthood because a small amount of Aqp2 protein can be expressed in the CD apical membrane.

The data from mice generated by floxing and excising an exon of the *Aqp2* gene are also generally consistent with lethality being associated with complete elimination of functional expression. For example, excision of exon 3 using a universally expressing Cre recombinase produces early lethality, whereas excision of this same exon using a Cre recombinase expressed only in the CD (and sparing the CNT) produces NDI without lethality at weaning (26). NDI mice produced by a tamoxifen-inducible Cre recombinase to excise exon 2 of *Aqp2* survive for at least several weeks after gene excision despite developing severe NDI and hydronephrosis (36). It seems likely that Cre-mediated recombination does not delete 100% of the targets (28). As a matter of fact, 1.5% and <5% of functional Aqp2 remain in the above two models (26,36), respectively, after Cre-mediated deletion. Thus it is possible that the remaining few percent of the cells that retain the ability to make the Aqp2 protein are sufficient to prevent lethality even though the phenotype represents severe NDI.

The reasons that mice with severe NDI die prematurely are probably the result of many factors, including serum hypertonicity, renal failure due to dehydration, and hydronephrosis. The time of onset and the severity of hydronephrosis could play an important role in the premature death of those mice. Mice with the S256L mutation in Aqp2 develop progressively severe hydronephrosis between 14 days and adulthood, but survive (17). In contrast, mice with a universally deleted exon 3 die within 14 days of birth with hydronephrosis. Thus the severity of the hydronephrosis correlates with mortality. The severity of the hydronephrosis is probably related to the magnitude of urine flow, which in turn is most likely inversely related to the degree of water reabsorption by the CD. Thus, from the available data, the most logical scenario to explain the magnitude of early mortality is the extent to which a small amount of functional Aqp2 can be expressed in the apical membrane of CD cells.

The role that Aqp2 in CNT plays in water homeostasis is still not clear. It was postulated that the rescuing of the lethal phenotype of Aqp2 knockout by the CD-specific deletion of *Aqp2* was the result of the CNT expression of Aqp2 (26), despite that fact that the Cre-mediated deletion of Aqp2 from CD was not complete. The result obtained from our mice and from the mice generated from tamoxifen-induced Cre-mediated deletion of exon 2 of *Aqp2* gene (36) seemed to be inconsistent with that explanation. With the low level of either the truncated or full-length Aqp2 expressed in both CD and CNT, the survival of these mice to adulthood seems to argue against a specific role for CNT-expressed Aqp2. Rather, the results are more consistent with the idea that a small amount of functional Aqp2 in CD and/or CNT is sufficient for affected mice to survive the neonatal period. This explanation was also consistent with mice with the F204V mutation in Aqp2 (15).

Although the severity of hydronephrosis might explain some of the difference in mortality in the mice expressing different types of Aqp2 mutations, it probably is not the complete explanation. Administration of water intraperitoneally at the time of weaning substantially improves mortality in our mice (Fig. 8). Administration of water should not reduce the magnitude of flow-induced hydronephrosis and renal failure. Administration of water also did not rescue the mice with the T126M mutation, the most severely affected of the reported Aqp2 mutants (35). Thus the magnitude of dehydration probably plays some role in survival during the nursing period and beyond. Dehydration and weakness during the weaning period might have affected the pups' ability to obtain enough water to maintain homeostasis, a situation that might have been alleviated by extra water administration, at least long enough to let the pups get enough strength to obtain water independently.

The expression of the Aqp2$^{\Delta 230}$ protein was lower in kidney CDs (Fig. 2 and Fig. 3) than in MDCK cells (Fig. 9). The reason for the marked reduction of the protein in the kidney is not clear. It is possible that the COOH-terminal truncation is processed differently in native CD cells than in MDCK cells. Another possibility is that the stably transfected MDCK cells have many more copies of *Aqp2* $^{\Delta 230}$ transgene incorporated into the cellular genome and thus higher expression of the truncated protein than the endogenous CD cells.

In summary, we have generated a mouse model of recessive NDI. The main features of this model are that the affected mice have severely reduced urine concentrating capacity, yet most of the affected mice survive the neonatal period, and majority of them survive to adulthood if water was administered at the time of weaning. For adult *Aqp2* $^{\Delta 230/\Delta 230}$ mice, the daily urine produced exceed their body weight, yet, with adequate hydration, those mice looked normal and both males and females were fertile. This mouse model demonstrates the important role of the COOH-terminal tail and the S256 residue in the apical translocation of Aqp2 in response to vasopressin stimulation. Thus this mouse model may be useful in studying the patho-physiology and potential therapy of this disease.

Acknowledgments

We thank Dr. P. Chambon (Institut de Genetique et de Biologie Moleculaire et Cellulaire, Illkirch, France) for providing the Cre-ER plasmid, Kathy Walters at the Central Microscopy Research Facility at the University of Iowa for excellent technical support, and Dr. P. Snyder at the University of Iowa for helpful discussion and technical assistance for this project. The skillful technical assistance of Joy Guo, Eileen Sweezer, and Thomas Kinney is gratefully acknowledged. The gene targeting and mouse husbandry were provided by the Gene Targeting Core Facility at the University of Iowa.

GRANTS

This work was supported by National Institute of Diabetes and Digestive and Kidney Diseases Grant P50 DK-52617 and a Merit grant from the Department of Veteran's Affairs.

REFERENCES

1. Cao XR, Shi PP, Sigmund RD, Husted RF, Sigmund CD, Williamson RA, Stokes JB, Yang B. Mice heterozygous for β-ENaC deletion have defective potassium excretion. Am J Physiol Renal Physiol. 2006; 291:F107–F115. [PubMed: 16571596]
2. Deen PM, Nielsen S, Bindels RJ, van Os CH. Apical and basolateral expression of aquaporin-1 in transfected MDCK and LLC-PK cells and functional evaluation of their transcellular osmotic water permeabilities. Pflugers Arch. 1997; 433:780–787. [PubMed: 9049170]
3. Deen PM, van Balkom BW, Kamsteeg EJ. Routing of the aquaporin-2 water channel in health and disease. Eur J Cell Biol. 2000; 79:523–530. [PubMed: 11001488]
4. Deen PM, Van Balkom BW, Savelkoul PJ, Kamsteeg EJ, Van Raak M, Jennings ML, Muth TR, Rajendran V, Caplan MJ. Aquaporin-2: COOH terminus is necessary but not sufficient for routing to the apical membrane. Am J Physiol Renal Physiol. 2002; 282:F330–F340. [PubMed: 11788448]

5. de Mattia F, Savelkoul PJ, Kamsteeg EJ, Konings IB, van der Sluijs P, Mallmann R, Oksche A, Deen PM. Lack of arginine vasopressininduced phosphorylation of aquaporin-2 mutant AQP2–R254L explains dominant nephrogenic diabetes insipidus. J Am Soc Nephrol. 2005; 16:2872–2880. [PubMed: 16120822]
6. Fujiwara TM, Bichet DG. Molecular biology of hereditary diabetes insipidus. J Am Soc Nephrol. 2005; 16:2836–2846. [PubMed: 16093448]
7. Fushimi K, Sasaki S, Marumo F. Phosphorylation of serine 256 is required for cAMP-dependent regulatory exocytosis of the aquaporin-2 water channel. J Biol Chem. 1997; 272:14800–14804. [PubMed: 9169447]
8. Glantz, SA. Primer of Biostatistics. New York: McGraw-Hill; 2002.
9. Jovov B, Wills NK, Lewis SA. A spectroscopic method for assessing confluence of epithelial cell cultures. Am J Physiol Cell Physiol. 1991; 261:C1196–C1203.
10. Kamsteeg EJ, Deen PM, van Os CH. Defective processing and trafficking of water channels in nephrogenic diabetes insipidus. Exp Nephrol. 2000; 8:326–331. [PubMed: 11014929]
11. Kamsteeg EJ, Heijnen I, van Os CH, Deen PM. The subcellular localization of an aquaporin-2 tetramer depends on the stoichiometry of phosphorylated and nonphosphorylated monomers. J Cell Biol. 2000; 151:919–930. [PubMed: 11076974]
12. Katsura T, Gustafson CE, Ausiello DA, Brown D. Protein kinase A phosphorylation is involved in regulated exocytosis of aquaporin-2 in transfected LLC-PK1 cells. Am J Physiol Renal Physiol. 1997; 272:F817–F822.
13. Kuwahara M, Iwai K, Ooeda T, Igarashi T, Ogawa E, Katsushima Y, Shinbo I, Uchida S, Terada Y, Arthus MF, Lonergan M, Fujiwara TM, Bichet DG, Marumo F, Sasaki S. Three families with autosomal dominant nephrogenic diabetes insipidus caused by aquaporin-2 mutations in the C-terminus. Am J Hum Genet. 2001; 69:738–748. [PubMed: 11536078]
14. Laycock JF, Hanoune J. From vasopressin receptor to water channel: intracellular traffic, constraint and by-pass. J Endocrinol. 1998; 159:361–372. [PubMed: 9834453]
15. Lloyd DJ, Hall FW, Tarantino LM, Gekakis N. Diabetes insipidus in mice with a mutation in aquaporin-2 (Abstract). PLoS Genet. 2005; 1:e20. [PubMed: 16121255]
16. Marr N, Bichet DG, Lonergan M, Arthus MF, Jeck N, Seyberth HW, Rosenthal W, van Os CH, Oksche A, Deen PM. Heteroligomerization of an Aquaporin-2 mutant with wild-type Aquaporin-2 and their misrouting to late endosomes/lysosomes explains dominant nephrogenic diabetes insipidus. Hum Mol Genet. 2002; 11:779–789. [PubMed: 11929850]
17. McDill BW, Li SZ, Kovach PA, Ding L, Chen F. Congenital progressive hydronephrosis (cph) is caused by an S256L mutation in aquaporin-2 that affects its phosphorylation and apical membrane accumulation. Proc Natl Acad Sci USA. 2006; 103:6952–6957. [PubMed: 16641094]
18. McDonald FJ, Yang B, Hrstka RF, Drummond HA, Tarr DE, McCray PB, Stokes JB, Welsh MJ, Williamson RA. Disruption of the beta subunit of the epithelial Na+ channel in mice: hyperkalemia and neonatal death associated with a pseudohypoaldosteronism phenotype. Proc Natl Acad Sci USA. 1999; 96:1727–1731. [PubMed: 9990092]
19. Mulders SM, Bichet DG, Rijss JP, Kamsteeg EJ, Arthus MF, Lonergan M, Fujiwara M, Morgan K, Leijendekker R, van der Sluijs P, van Os CH, Deen PM. An aquaporin-2 water channel mutant which causes autosomal dominant nephrogenic diabetes insipidus is retained in the Golgi complex. J Clin Invest. 1998; 102:57–66. [PubMed: 9649557]
20. Mulders SM, Knoers NV, Van Lieburg AF, Monnens LA, Leumann E, Wuhl E, Schober E, Rijss JP, Van Os CH, Deen PM. New mutations in the AQP2 gene in nephrogenic diabetes insipidus resulting in functional but misrouted water channels. J Am Soc Nephrol. 1997; 8:242–248. [PubMed: 9048343]
21. Nielsen S, Frokiaer J, Marples D, Kwon TH, Agre P, Knepper MA. Aquaporins in the kidney: from molecules to medicine. Physiol Rev. 2002; 82:205–244. [PubMed: 11773613]
22. Nishimoto G, Zelenina M, Li D, Yasui M, Aperia A, Nielsen S, Nairn AC. Arginine vasopressin stimulates phosphorylation of aquaporin-2 in rat renal tissue. Am J Physiol Renal Physiol. 1999; 276:F254–F259.

23. Noda Y, Sasaki S. Molecular mechanisms and drug development in aquaporin water channel diseases: molecular mechanism of water channel aquaporin-2 trafficking. J Pharmacol Sci. 2004; 96:249–254. [PubMed: 15539762]
24. Noda Y, Sasaki S. Trafficking mechanism of water channel aquaporin-2. Biol Cell. 2005; 97:885–892. [PubMed: 16293109]
25. Preston GM, Carroll TP, Guggino WB, Agre P. Appearance of water channels in Xenopus oocytes expressing red cell CHIP28 protein. Science. 1992; 256:385–387. [PubMed: 1373524]
26. Rojek A, Fuchtbauer EM, Kwon TH, Frokiaer J, Nielsen S. Severe urinary concentrating defect in renal collecting duct-selective AQP2 conditional-knockout mice. Proc Natl Acad Sci USA. 2006; 103:6037–6042. [PubMed: 16581908]
27. Sands JM, Bichet DG. Nephrogenic diabetes insipidus. Ann Intern Med. 2006; 144:186–194. [PubMed: 16461963]
28. Schwenk F, Kuhn R, Angrand PO, Rajewsky K, Stewart AF. Temporally and spatially regulated somatic mutagenesis in mice. Nucleic Acids Res. 1998; 26:1427–1432. [PubMed: 9490788]
29. Sohara E, Rai T, Yang SS, Uchida K, Nitta K, Horita S, Ohno M, Harada A, Sasaki S, Uchida S. Pathogenesis and treatment of autosomal-dominant nephrogenic diabetes insipidus caused by an aquaporin 2 mutation. Proc Natl Acad Sci USA. 2006; 103:14217–14222. [PubMed: 16968783]
30. Tamarappoo BK, Yang B, Verkman AS. Misfolding of mutant aqua-porin-2 water channels in nephrogenic diabetes insipidus. J Biol Chem. 1999; 274:34825–34831. [PubMed: 10574954]
31. Valenti G, Procino G, Tamma G, Carmosino M, Svelto M. Minireview: aquaporin 2 trafficking. Endocrinology. 2005; 146:5063–5070. [PubMed: 16150901]
32. van Balkom BW, Graat MP, van Raak M, Hofman E, van der Sluijs P, Deen PM. Role of cytoplasmic termini in sorting and shuttling of the aquaporin-2 water channel. Am J Physiol Cell Physiol. 2004; 286:C372–C379. [PubMed: 14561591]
33. van Lieburg AF, Verdijk MA, Knoers VV, van Essen AJ, Proesmans W, Mallmann R, Monnens LA, van Oost BA, van Os CH, Deen PM. Patients with autosomal nephrogenic diabetes insipidus homozygous for mutations in the aquaporin 2 water-channel gene. Am J Hum Genet. 1994; 55:648–652. [PubMed: 7524315]
34. van Os CH, Deen PM. Aquaporin-2 water channel mutations causing nephrogenic diabetes insipidus. Proc Assoc Am Physicians. 1998; 110:395–400. [PubMed: 9756089]
35. Yang B, Gillespie A, Carlson EJ, Epstein CJ, Verkman AS. Neonatal mortality in an aquaporin-2 knock-in mouse model of recessive nephrogenic diabetes insipidus. J Biol Chem. 2001; 276:2775–2779. [PubMed: 11035038]
36. Yang B, Zhao D, Qian L, Verkman AS. Mouse model of inducible nephrogenic diabetes insipidus produced by floxed aquaporin-2 gene deleltion. Am J Physiol Renal Physiol. 2006; 291:F465–F472. [PubMed: 16434568]

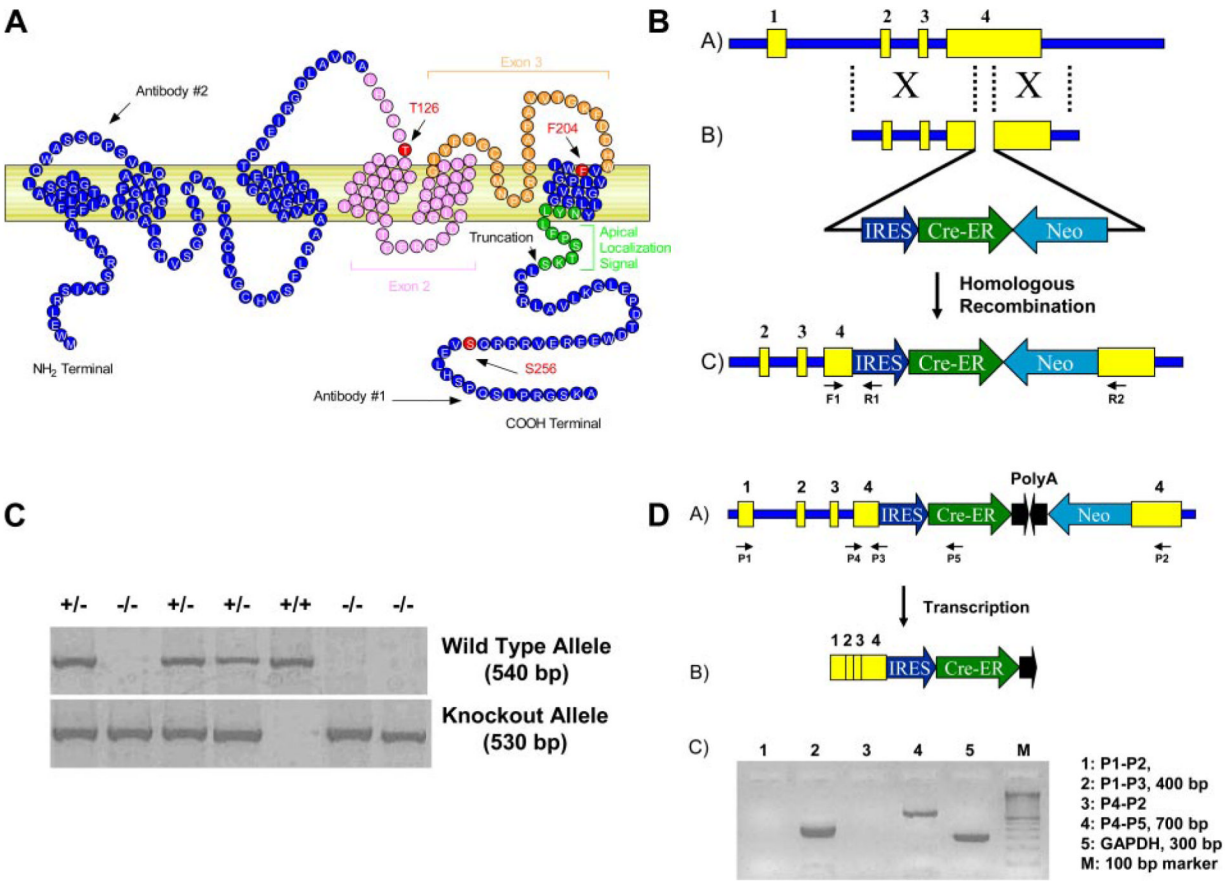

Fig. 1.

Generation of mice with COOH-terminal truncation of the aquaporin (Aqp)-2 water channel. *A*: schematic drawing of mouse Aqp2. The locations of S256 and the putative apical localization signal and the truncation site are marked. Two different antibodies were used in this study, and the approximate epitope locations are marked as well. Several published Aqp2 mice, the T126M knock-in, the floxing of *exons 2* and *3*, and the F204 are also indicated. *B*: schematic drawing of the gene targeting to generate Aqp2 truncation. Neo-selectable marker, along with Cre-endoplasmic reticulum (ER) coding region, was inserted into *exon 4* of mouse *Aqp2* gene through homologous recombination. *C*: genotyping of a litter of mice obtained from intercross of heterozygotes for the truncation of *Aqp2* (*Aqp2* $^{\Delta 230/+}$). *D*: RT-PCR analyses using total RNA isolated from kidney of mice homozygous for the deletion (*Aqp2* $^{\Delta 230/\Delta 230}$). Data show no expression of the distal portion of *exon 4* (*lanes 1* and *3*) but expression of the proximal portion of *exon 4* (*lanes 2* and *4*) with expression of the message for Cre recombinase (*lane 4*).

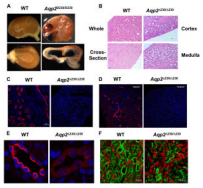

Fig. 2.

Kidney histology and immunohistology of *Aqp2* $^{\Delta 230/\Delta 230}$ mice. Kidneys were collected from mice of different genotypes at 4 wk of age. *A*: gross kidney appearance is shown. *B*: hematoxylin and eosin staining of kidney is shown. Immunostainings using antibodies against the COOH-terminal (*C*) and NH_2-terminal (*D*) regions of Aqp2 are shown. *E:* higher magnification of images in *D. F*: immunostainings using antibodies against AQP3.

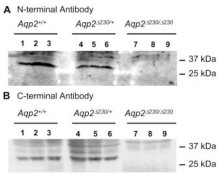

Fig. 3.

Western blot to detect Aqp2 protein in the kidney. Kidneys from 3 mice each of wild-type (WT), heterozygotes, and homozygous *Aqp2* $^{\Delta 230/\Delta 230}$ mice were used for protein analysis. Equal amount of protein was loaded in each lane and probed with either primary antibody against the NH_2-terminal (*A*) and COOH-terminal (*B*) regions of Aqp2.

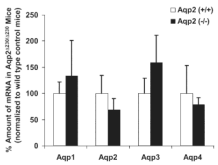

Fig. 4.

Real-time PCR. Total kidney RNA, from 3 WT control and 3 *Aqp2* $^{\Delta 230/\Delta 230}$ mice, was used for real-time RT-PCR analyses. Glyceraldehyde-3-phosphate dehydrogenase (GAPDH) was used as internal control. The relative amount of transcript was expressed as a percentage of that of WT. There are no significant differences between any of the Aqps.

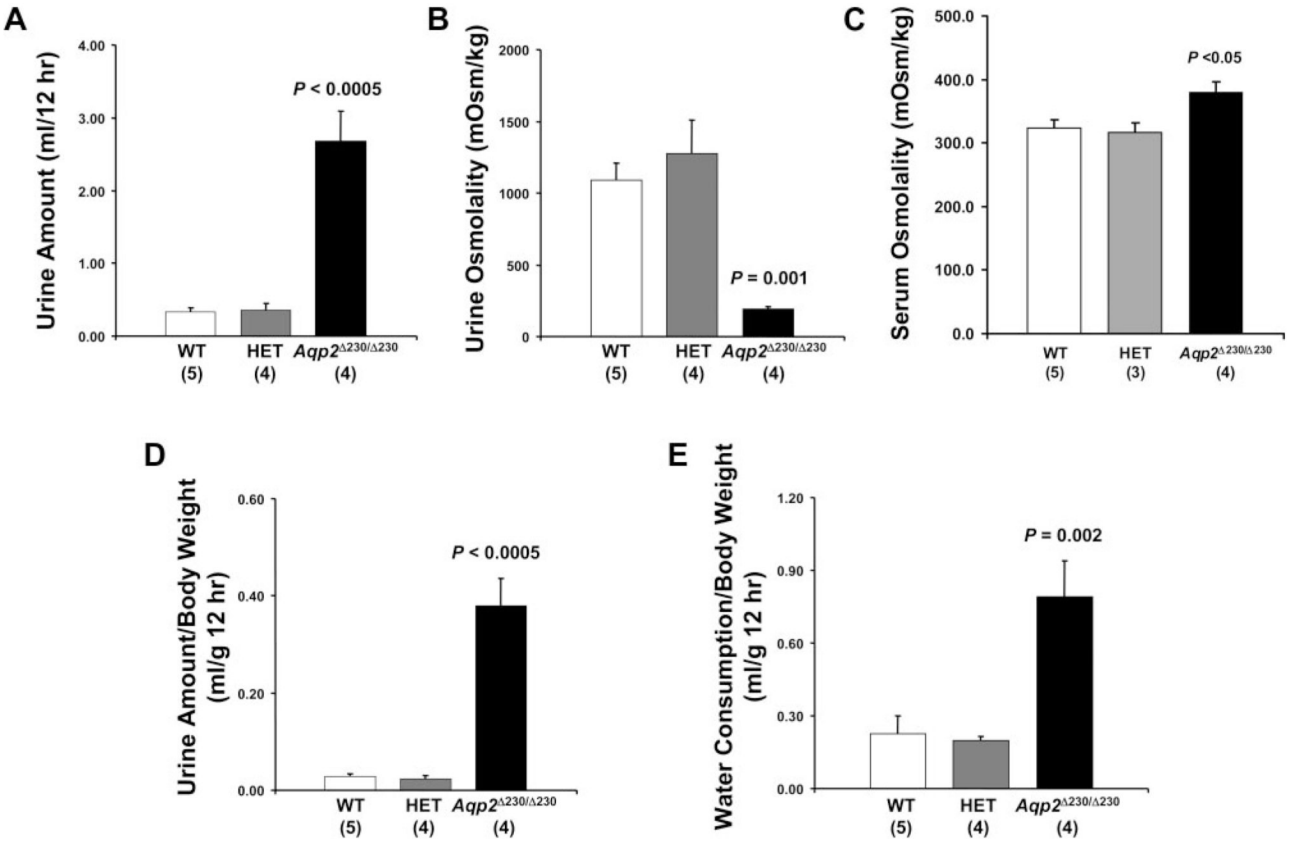

Fig. 5.

Aqp2 $^{\Delta 230/\Delta 230}$ mice have reduced urine concentrating capacity. Four-week-old littermates of all 3 genotypes (WT, HET, and *Agp2* $^{\Delta 250/\Delta 250}$) were placed in metabolic cages for 12 h (8:00 P.M. to 8:00 A.M.) with free access of drinking water. Urine volume (*A*) and osmolality (*B*) and serum osmolality (*C*) were measured and plotted. The amount of urine collected and water consumed during the collection period was normalized with body weight (*D* and *E*). No. of animals in each group is shown in parentheses.

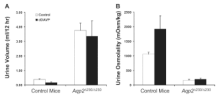

Fig. 6.

Aqp2 $^{\Delta 230/\Delta 230}$ mice are resistant to the stimulation of vasopressin. Four-week-old mice were given desmopressin (dDAVP) ip at a dosage of 1 μg/kg of body wt before being placed in metabolic cages. Urine volume (*A*) and osmolality (*B*) show that control mice respond to dDAVP while *Aqp2* $^{\Delta 230/\Delta 230}$ do not. There were 4 nephrogenic diabetes insipidus (NDI) mice and 9 control mice (both WT and HET) used in this study.

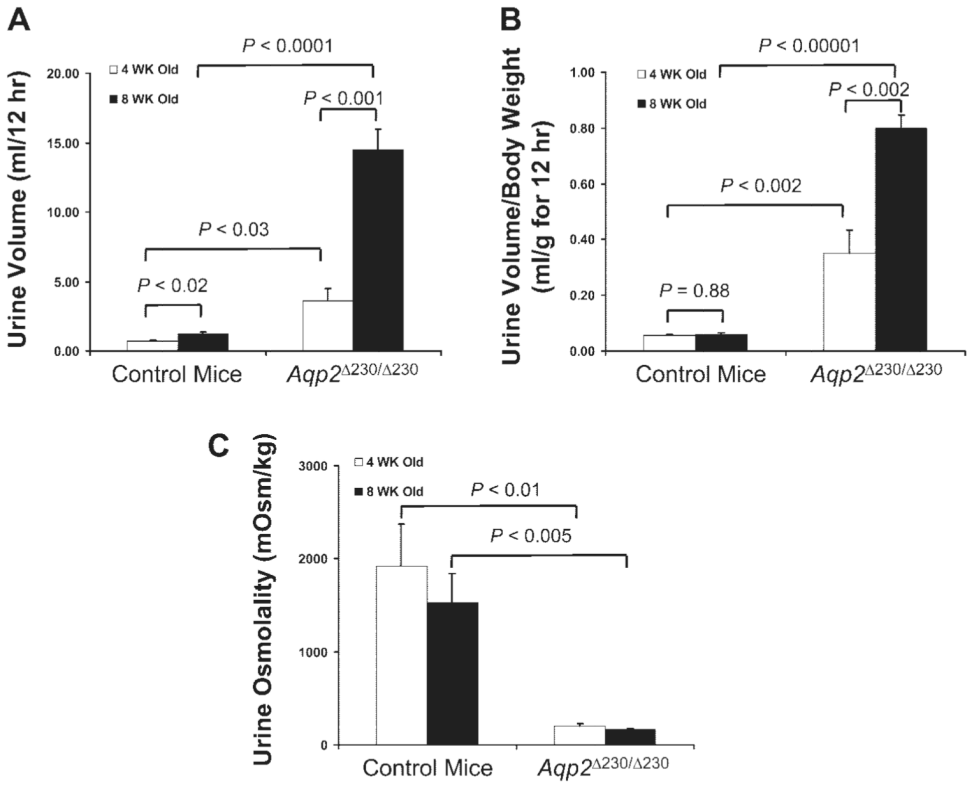

Fig. 7.

Age-dependent change in *Aqp2* $^{\Delta 230/\Delta 230}$ mice. The same groups of mice used in initial study at 4 wk (Fig. 2) were further tested at 8 wk. The amount of urine produced (*A*) and the amount of urine normalized to body weight (*B*) and osmolality are shown. There were 4 NDI mice and 9 control mice (both WT and HET) used in this study.

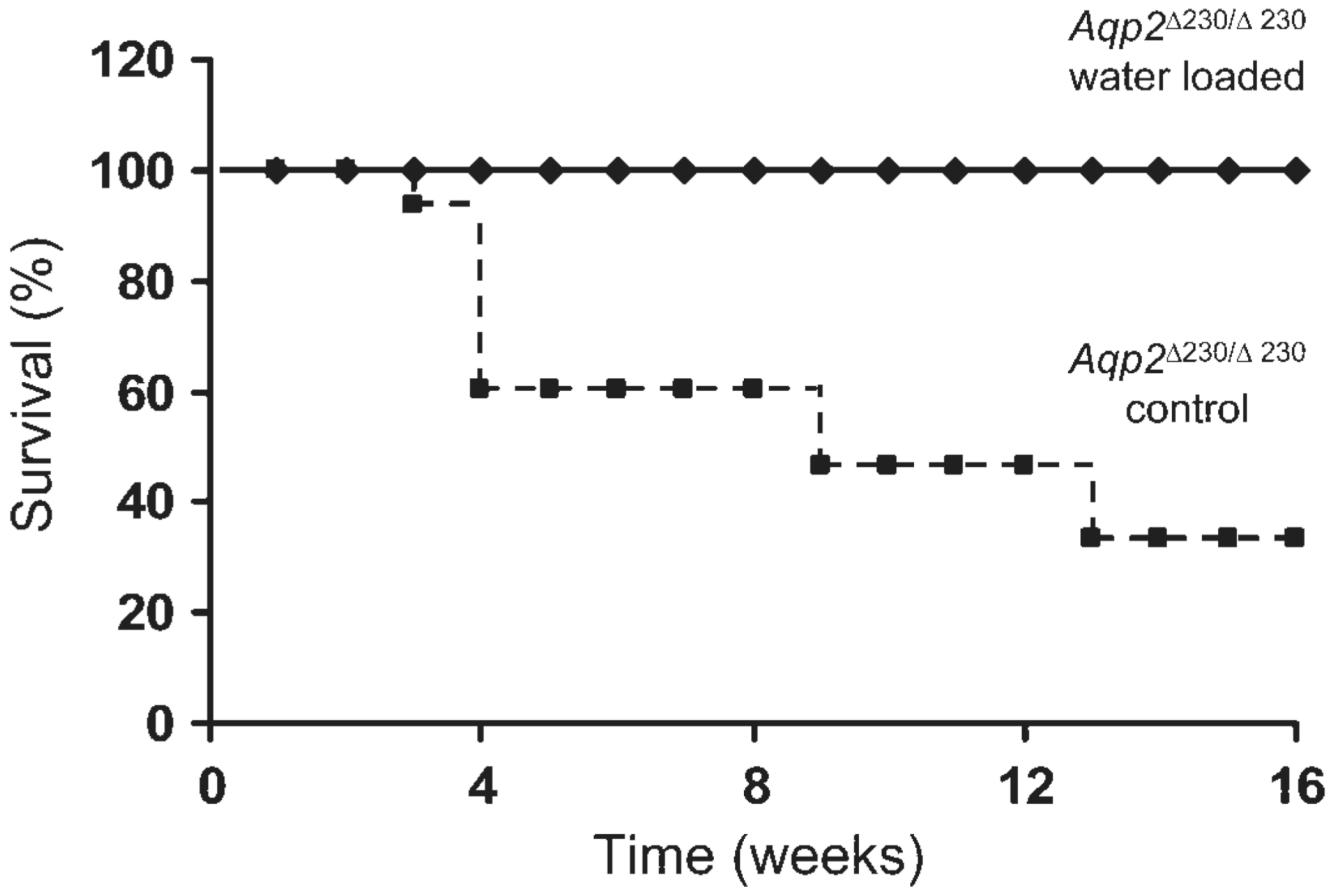

Fig. 8.

Water loading improved survival for *Aqp2* $^{\Delta 230/\Delta 230}$ mice. *Aqp2* $^{\Delta 230/\Delta 230}$ weanlings (21 days old) were given a single ip injection of water (volume = 10% of body weight). Time of death was recorded. Kaplan-Meier survival curves are shown. There were 5 *Aqp2* $^{\Delta 230/\Delta 230}$ mice in the water-load group and 16 *Aqp2* $^{\Delta 230/\Delta 230}$ mice in the control group, without acute water loading.

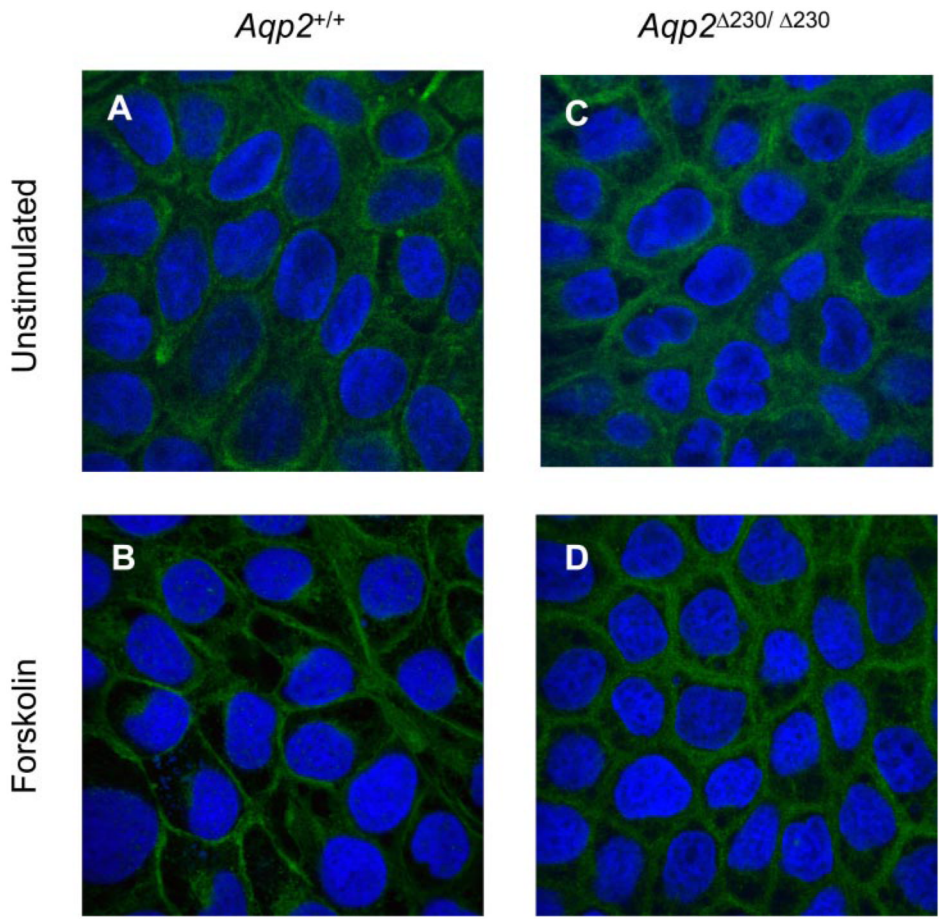

Fig. 9.

Stable transfection of MDCK cells showed that Aqp2$^{\Delta 230}$ can reach the plasma membrane. MDCK cells were stably transfected with plasmids containing full-length Aqp2 cDNA (*A* and *B*) and Δ230 truncation (*C* and *D*). Cells were cultured in the absence (*A* and *B*) or in the presence (*B* and *D*) of forskolin (10 μM) for 2 h. Cells were fixed, and Aqp2 was visualized with anti-Aqp2 (NH_2 terminal, rabbit antiserum) and fluorescence-labeled secondary goat anti-rabbit IgG.

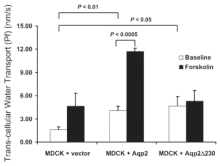

Fig. 10.

Transcellular water transport (Pf) in MDCK cells. MDCK cells were stably transfected with control plasmid and plasmids containing cDNA coding for either full-length or Δ230 truncation of Aqp2. Cells were seeded on Transwells and used for Pf study using a spectroscopic method to determine the phenol red concentration. Pf is expressed as nm/s. Average from 3 experiments is shown with SE.

Table 1

Body weight, creatinine, and BUN of $Aqp2^{\Delta 230/\Delta 230}$ mice

	Body Wt, g			
	3wk	10wk	Creatinine, mg/dl	BUN, mg/dl
WT	11.1±0.6 (8)	23.16±1.55 (9)	0.04±0.01 (4)	14.3±0.7 (4)
HET	11.1 ±0.3 (8)	23.63±0.6 (3)	0.04±0.01 (4)	13.8±0.5 (4)
Aqp2$^{\Delta 230/\Delta 230}$	8.7±1.7*(5)	17.49±1.66f† (4)	0.05±0.00 (4)	37.5±13.3*(4)

Values represent means ± SE; no. of mice parentheses, BUN, blood urea nitrogen; WT, wild type; Aqp, aquaporin. There was no statistical difference between HET and WT mice

$^{*}P < 0.05$

$^{\dagger}P < 0.01$ between *Aqp2*$^{\Delta 230/\Delta 230}$ mice and control mice (HET and WT together).